Periodico di Mineralogia (2012), 81, 1, 75-92 DOI: 10.2451/2012PM0005

PERIODICO di MINERALOGIA
established in 1930

An International Journal of
MINERALOGY, CRYSTALLOGRAPHY, GEOCHEMISTRY,
ORE DEPOSITS, PETROLOGY, VOLCANOLOGY
and applied topics on *Environment*, *Archeometry* and *Cultural Heritage*

Pumpellyite veins in the metadolerite of the Frido Unit (Southern Apennines - Italy)

Maria T. Cristi Sansone[1,*] and Giovanna Rizzo[2]

[1] Dipartimento di Scienze Geologiche, Università della Basilicata, 85100 Potenza, Italy
[2] Dipartimento di Chimica, Università della Basilicata, 85100 Potenza, Italy
* Corresponding author: *mariacristisansone@virgilio.it*

Abstract

This study focuses on pumpellyite veins cross-cutting the metadolerites of the Frido Unit Ophiolites (Southern Apennines - Italy). Pumpellyite occurs in the metadolerites as felt-radiated aggregates or prism filling veins; metadolerites show mineral assemblages of the prehnite–pumpellyite and lawsonite-glaucophane metamorphic facies. Texture and composition of minerals in these veins are heterogeneous as revealed by SEM and EMPA characterisations, respectively. Either in the host rocks and in the veins, mineral compositions indicate a polyphase metamorphic evolution; these metadolerites recorded both the ocean-floor metamorphism and their emplacement within the Liguride accretionary wedge (HP/LT). In particular, the Fe and Mg amounts in the pumpellyite crystallised in the veins ranges between 0.216 - 0.585 and 0.293 - 0.466 apfu, respectively, whereas Al ranges between 2.518 - 2.802 apfu. These compositional variations reflect a similar metamorphic evolution of the host rock and pumpellyite veins of the Frido Unit.

Key words: Southern Apennines; Frido Unit; ophiolites; metadolerites; veins; pumpellyite.

Introduction

The ophiolitic sequences outcropping in the Southern Apennines, are remnants of the Ligurian oceanic lithosphere pertaining to the Jurassic western Tethys. The Liguride Units include sequences characterized by high pressure/low temperature (hereafter HP/LT) (Lanzafame et al., 1979; Spadea, 1982) metamorphic overprint in the Frido Unit (Vezzani, 1969; 1970) and sequences lacking orogenic metamorphism in the North-Calabria Unit (Bonardi et al., 1988).

In this study, the veins hosted in the metadolerites of the Frido Unit (San Severino Lucano, Southern Apennines) has been investigated by optical microscopy, SEM, EMPA and XRF methods.

These metadolerites dikes intruded serpentinized peridotites and developed different textures, from intersertal to grano-xenoblastic to mylonitic with increasing metamorphic effects (Sansone et al., 2011). Metadolorites record various degrees of metamorphic re-crystallization: an ocean-floor metamorphism and an orogenic overprint (Sansone et al., 2011); the ocean-floor metamorphism often occured with metasomatic processes of rodingitization (typical of dike-cut serpentinite) and spilitization (Hellman and Henderson, 1977); rodingitization produces Ca-rich basic rocks during serpentinization (Paulick et al., 2006; Sansone et al., 2011).

The different types of veins of the Frido Unit host both non-fibrous and fibrous minerals; their crystal assemblages mainly consist of pumpellyite and subordinately smaller amounts of other minerals, such as chlorite + prehnite + plagioclase + tremolite + actinolite + white mica + quartz + calcite + albite + epidote + glaucophane + lawsonite and + chrysotile. Here, we extended previous results on the metamorphic evolution of the Frido Unit by a careful investigation of the pumpellyite crystal-chemical variations, mainly defined by the Al-Fe^{3+} substitution (Ishizuka, 1991), potentially able to constrain the metamorphic evolution in the zeolite, prehnite-pumpellyite, pumpellyite-actinolite and blueschist facies.

In general, Fe-pumpellyite crystallises under lower-grade metamorphic conditions than Al-pumpellyite (Ernst et al., 1970; Coombs et al., 1976; Mével, 1981). In the Frido Unit Ophiolites, pumpellyite occurs in the metadolerites affected by ocean-floor rodingitic alteration (Sansone et al., 2011). Our aim is to relate the compositional variation of pumpellyite in metadolerites of the ophiolitic Frido Unit and its relations with respect the host rock composition and metamorphic conditions.

Ophiolites in the Southern Apennines

The Southern Apennines fold-and-thrust mountain belt (Figure 1) formed between upper Oligocene and Quaternary (Patacca and Scandone, 2007 and references therein) as the

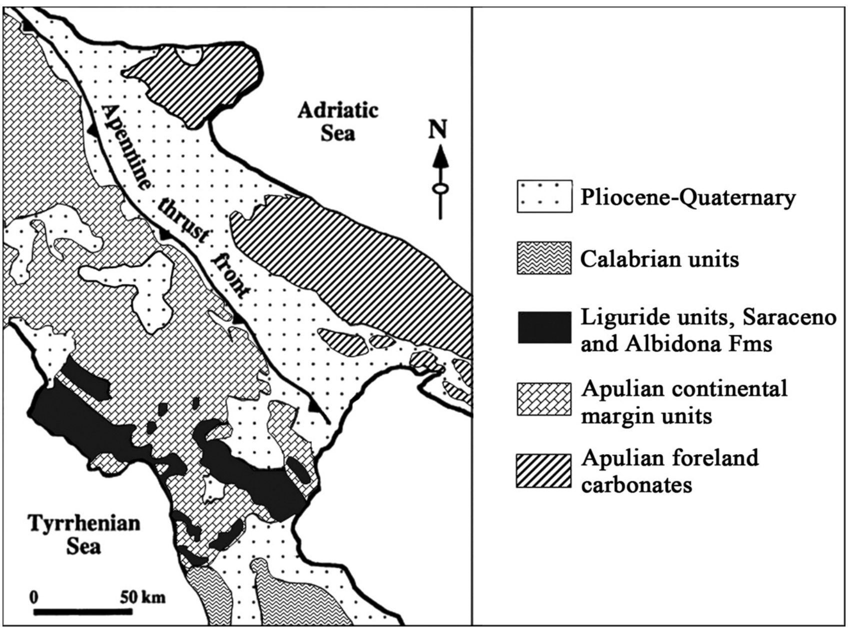

Figure 1. Geological sketch map of the Southern Apennines, modified after Mazzoli (1998).

result of the convergence between the African and European plates and simultaneous rollback SE-directed by the Ionian subduction (Cello and Mazzoli, 1999; Doglioni et al., 1999; Gueguen et al., 1998).

The Apenninic accretionary prism is issued from a northward subduction of an Alpine Tethys (Stampfli et al., 2002) sea-floor remnant, also known as western Tethys (Bortolotti and Principi, 2005), beneath European plate since Oligocene times.

The Liguride Units include both sequences characterized by HP/LT metamorphic overprint such as the Frido Unit (Vezzani, 1969) and sequences devoid of orogenic metamorphism such as the North Calabria Unit (Bonardi et al., 1988).

Ogniben (1969), Knott (1987; 1994), Monaco et al. (1991) and Tortorici et al. (2009) considered the Liguride Units as suture zones related to the closure of the western Tethys oceanic domain with the European plate (Calabride units) and the African plate. Knott (1987; 1994), Monaco et al. (1991), and Monaco and Tortorici (1995) suggested that metamorphism and deformation of these units took place in an accretionary wedge. In this setting, the Frido Unit has been interpreted as part of an accretionary wedge developed during the NW-oriented subduction of the Ligurian sector of the Tethyan Ocean since the Late Cretaceous age (Knott, 1987; 1994). According to Amodio-Morelli et al. (1976) and Bonardi et al. (1988), the metamorphic Liguride Units are analogous to elements of the eo-alpine chain with a European vergence later included in the Apennines Chain.

The ophiolitic rocks occurring in the very low-grade Frido Unit (Vezzani, 1970) consist of serpentinites derived from a lherzolite mantle and subordinately harzburgites. The serpentinites are frequently associated to tectonic slices made of diabase and medium- to high-grade metamorphic rocks such as amphibolites, gneiss, granofels as well as meta- Fe-gabbros and metabasalts with relic pillow structures (Lanzafame et al., 1979; Spadea, 1979; 1982; 1994). Ophiolite sequences show a NE vergence in the Southern Apennines (Knott, 1987; 1994; Monaco, 1993).

Sampling and analytical methods

Thirty-five samples of metadolerites from the Frido Unit were collected near the village of San Severino Lucano (Basilicata region, Southern Italy) (Figure 2).

Preliminary petrographic characterisation of all the thirty-five samples was carried out with an optical microscopy on oriented rock samples as a function of their foliations and lineations (Table 1).

Then, major element bulk composition was carried out on nineteen selected samples of metadolerites (Table 2), using a PHILIPS PW-1480 XRF spectrometer installed at the Department of Earth Sciences, University of Calabria; XRF data were corrected according to the protocols of Franzini et al. (1972; 1975) and Leoni and Saitta (1976).

The micro-chemical composition of minerals was obtained with a CAMECA SX-50 equipped with four WDS spectrometers (Tables 3, 6) and one EDS electron microprobe at the Istituto di Geoscienze e Georisorse (IGG) of the CNR (Padua, Italy); the analytical conditions were: 15 kV accelerating voltage and 15 nA beam current, count time 10 s at peak and 5 s at background. Natural and synthetic oxides and silicate minerals were used as standards. Data were treated using the classical PAP analytical procedure.

SEM-EDS analyses were performed at the Department of Earth Sciences, University of Calabria (Arcavacata di Rende, Cosenza, Italy), using a FEI/Philips scanning microscope with GENESIS-4000 EDAX X-ray system based on a Si/Li crystal detector.

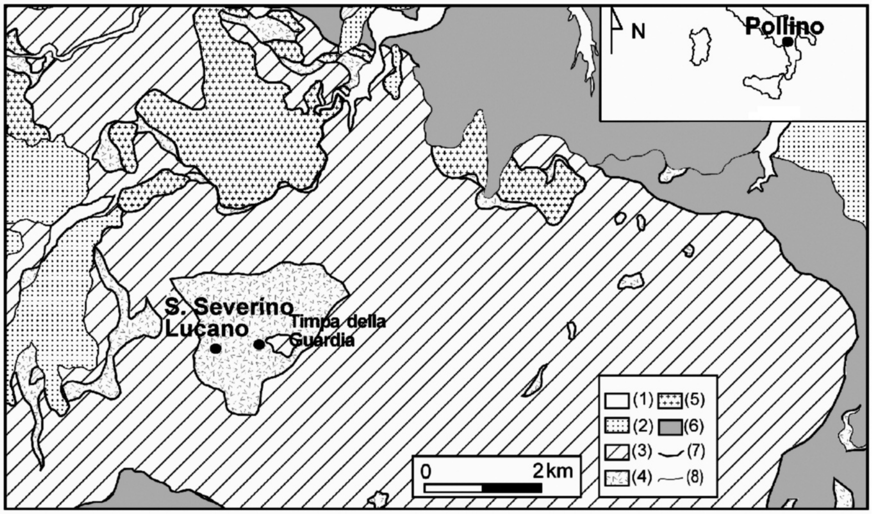

Figure 2. Geological map of the Liguride Unit cropping out near Pollino Ridge (Sansone et al., 2011, modified after Monaco et al., 1995). (1) Alluvial deposits; (2) Pleistocene deposits; (3) Frido Unit; (4) Ophiolites; (5) Amphibolites, gneiss, and granofels; (6) North-Calabrian Unit; (7) Faults; (8) Stratigraphic limit.

We adopted the symbols for minerals recommended by Siivola and Schmid (2007), excepting for the following symbols: bl Am*(blue amphibole), gr Am*(green amphibole), br Am*(brown amphibole), Olg*(oligoclase), wht Mca*(white mica) (see Table 1).

Results and Discussion

Petrography of the host rocks

The mineral assemblage in each metadolorite are reported in Table 1, the bulk chemical compositions of the 19 selected samples are reported in Table 2, whereas the composition of pyroxene, amphibole, plagioclase and pumpellyite phases are shown in Tables 3, 4, 5 and 6, respectively.

Metadolerites present different kinds of texture: intersertal, blastophitic, and a mylonitic fabric (Figure 3a, b). Opaque minerals, Fe-hydroxides, zircon, and spinel occur as accessory phases. Metadolerites are cut by veins (Figure 3c) filled with pumpellyite and ± chlorite ± prehnite ± plagioclase ± tremolite ± actinolite ± white mica ± quartz ± calcite ± albite ± epidote ± lawsonite ± glaucophane and ± chrysotile.

The petrographical features allowed us to subdivide the metadolerites into three different types depending on oceanic and/or orogenic metamorphic mineral assemblages (Table 1):

1) Rocks with Pl and Cpx have an intersertal, blastophitic texture or a mylonitic fabric and at times a seriate texture (Type A). Some samples (Type A*) have a high content of prehnite whose crystals occur in cataclastic-mylonitic bands (Sansone et al., 2011).

2) Rocks with Pl, Cpx, and brown Hbl show an intersertal or a blastophitic texture (Type B) (Sansone et al., 2011).

3) Rocks with Pl, Cpx, brown Hbl, and blue Amph have an intersertal or a blastophitic texture (Type C) (Sansone et al., 2011).

Original magmatic plagioclase (PL1) (Table 5) in the matrix is completely sericitized and

Table 1. Magmatic and metamorphic assemblages of the metadolerites.

Sample	Magmatic assemblage	Metamorphic minerals	Type
MC2	Pl1 + Cpx	Chl ± gr Am* ± Pmp ± Qtz ± Prh ± wht Mca*	A
MC3	Pl1 + Cpx	Br Am* +Chl ± Pmp ± wht Mca* ± Qtz ± Prh ± gr Am*	B
MC6	Pl1 + Cpx	Br Am* +Chl ± Pmp ±wht Mc*± Qtz ± Prh ± gr Am*	B
MC14	Pl1 + Cpx	Chl ± gr Am* ± Pmp ± Qtz ± Prh ± wht Mca*	A
MC18	Pl1 + Cpx	Chl ± gr Am* ± Pmp ± Qtz ± Prh ± wht Mca*	A
MC20	Pl1 + Cpx	Chl ± gr Am* ± Pmp ± Qtz ± Prh ± wht Mca*	A
MC23	Pl1 + Cpx	Br Am* + Chl ± Pmp ± wht Mca* ± Qtz ± Prh ± gr Am*	B
MC25	Pl1 + Cpx	Prh + Chl ± Qtz ± wht Mca* ± Pmp ± Srp*	A*
MC29	Pl1 + Cpx	Br Am* + Chl ± Pmp ± wht Mca* ± Qtz ± Prh ± gr Am*	B
MC31	Pl1 + Cpx	Br Am* + Chl ± Pmp ± wht Mca*± Qtz ± Prh ±gr Am*	B
MC32a	Pl1 + Cpx	Br Am* + Chl ± Pmp ± wht Mca* ± Qtz ± Prh ± gr Am*	B
MC33	Pl1 + Cpx	Prh + Chl ± Qtz ± wht Mca* ± Pmp ± Srp*	A*
MC35	Pl1 + Cpx	Chl ± gr Am* ± Pmp ± Qtz ± Prh ± wht Mca*	
MC38	Pl1 + Cpx	Chl ± gr Am* ± Pmp ± Qtz ± Prh ± wht Mca*	A
MC40	Pl1 + Cpx	Ab (Pl3) +Olg* (Pl2) +br Am* + Qtz + Chl + bl Am* ± Lws ± wht Mca* ± Prh	C
MC42	Pl1 + Cpx	Br Am* + Chl ± Pmp ± wht Mca* ± Qtz ± Prh ± gr Am*	B
MC45	Pl1 + Cpx	Br Am* +Chl ±Pmp ± wht Mca* ± Qtz ±Prh ± gr Am*	B
MC49	Pl1 + Cpx	Chl ± gr Am* ± Pmp ± Qtz ± Prh ± wht Mca*	A
MC51	Pl1 + Cpx	Br Am* + Chl ± Pmp ± wht Mca* ± Qtz ± Prh ± gr Am*	B
MC59	Pl1 + Cpx	Chl ±gr Am* ± Pmp ± Qtz ± Prh ± wht Mca*	A
MC60	Pl1 + Cpx	Br Am* + Chl ±Pmp ± wht Mca* ± Qtz ± Prh ± gr Am*	B
MC61	Pl1 + Cpx	Br Am* +Chl ± Pmp ± wht Mca* ± Qtz ± Prh ± gr Am*	B
MC62	Pl1 + Cpx	Br Am* +Chl ±Pmp ±wht Mc* ±Qtz ±Prh ±gr Am*	B
MC65	Pl1 + Cpx	Br Am* + Chl ±Pmp ± wht Mca* ± Qtz ± Prh ± gr Am*	B
MC68	Pl1 + Cpx	Br Am* + Chl ± Pmp ± wht Mca* ±Qtz ±Prh ±gr Am*	B
MC69	Pl1 + Cpx	Ab (Pl3) +Olg* (Pl2) +br Am* +Qtz +Chl +bl Am*± Lws ± wht Mca* ± Prh	C
MC70	Pl1 + Cpx	Ab (Pl3) +Olg* (Pl2) +br Am* +Qtz +Chl +bl Am* ±Lws ±wht Mc* ±Prh	C
MC71	Pl1 + Cpx	Br Am* + Chl ± Pmp ± wht Mca* ± Qtz ± Prh ± gr Am*	B
MC72	Pl1 + Cpx	Br Am* + Chl ± Pmp ± wht Mca* ± Qtz ± Prh ± gr Am*	B
MC73	Pl1 + Cpx	Br Am* + Chl ± Pmp ± wht Mca* ± Qtz ± Prh ± gr Am*	B
MC74	Pl1 + Cpx	Chl ± gr Am* ± Pmp ± Qtz ± Prh ± wht Mca*	A
MC75	Pl1 + Cpx	Br Am* + Chl ± Pmp ± wht Mca* ± Qtz ± Prh ± gr Am*	B
MC76	Pl1 + Cpx	Br Am* + Chl ± Pmp ± wht Mca* ± Qtz ± Prh ± gr Am*	B
MC77	Pl1 + Cpx	Ab (Pl3) + Olg* (Pl2) + br Am* + Qtz + Chl + bl Am*±Lws ± wht Mca* ± Prh	C
MC78	Pl1 + Cpx	Prh + Chl ± Qtz ± wht Mca* ± Pmp ± Srp*	A*

bl Am*(blue amphibole), gr Am*(green amphibole), br Am*(brown amphibole), Olg*(oligoclase), wht Mca*(white mica)

Table 2. Bulk rock chemistry of metadolerites.

Sample	MC51	MC49	MC45	MC42	MC40	MC38	MC35	MC33	MC32A	MC31	MC29	MC25	MC23	MC20	MC18	MC14	MC6	MC3	MC2
Oxides (wt %)																			
SiO_2	39.59	39.03	43.41	37.87	44.98	37.70	38.95	30.96	40.95	39.74	39.63	31.80	38.32	37.66	41.31	37.65	46.97	38.25	37.75
TiO_2	1.81	1.67	1.45	1.62	1.4	1.01	0.83	0.80	1.08	1.05	1.07	0.66	1.73	1.74	0.97	1.00	1.48	2.27	1.61
Al_2O_3	14.38	14.42	15.7	16.43	16.98	15.4	18.4	17.78	14.91	14.88	14.06	13.97	14.2	13.19	15.81	15.93	16.81	14.46	13.18
Fe_2O_3	11.05	11.18	9.53	9.77	9.30	10.27	7.00	8.44	9.82	9.28	9.29	9.33	10.85	10.42	9.66	10.49	9.36	11.24	10.01
MnO	0.17	0.17	0.15	0.22	0.14	0.20	0.15	0.21	0.17	0.20	0.19	0.31	0.15	0.15	0.14	0.18	0.13	0.19	0.18
MgO	11.08	11.87	10.25	10.57	9.26	13.69	10.23	26.83	13.52	13.97	15.1	30.95	10.73	15.26	14.87	13.45	9.08	11.56	16.00
CaO	16.81	16.19	12.83	17.65	9.90	16.36	18.5	5.80	13.61	15.30	15.55	2.86	19.26	15.97	8.88	15.33	7.58	16.46	15.65
Na_2O	0.46	0.44	1.85	0.48	2.45	0.10	0.19	n.d.	1.03	0.39	0.19	n.d.	0.16	0.16	2.11	0.32	3.47	0.40	0.14
K_2O	0.03	0.02	0.75	0.02	1.48	n.d.	n.d.	n.d.	0.23	0.12	n.d.	n.d.	n.d.	n.d.	0.40	n.d.	1.36	0.03	n.d.
P_2O_5	0.24	0.19	0.17	0.21	0.18	0.08	0.09	0.08	0.11	0.11	0.12	0.05	0.22	0.24	0.08	0.09	0.17	0.35	0.23
LOI	4.38	4.82	3.91	5.15	3.94	5.19	5.66	9.11	4.57	4.97	4.79	10.07	4.38	5.22	5.78	5.57	3.59	4.79	5.24

n.d. not-detected

Table 3. Representative analyses of clinopyroxene.

Sample	MC40	MC40	MC40	MC40
N. Analysis	11	12	13	14
Oxides (wt%)	rim	core	core	rim
SiO_2	51.89	48.74	51.30	50.96
TiO_2	1.21	1.67	1.03	1.20
Al_2O_3	4.27	6.70	4.76	4.77
Cr_2O_3	0.04	0.18	0.75	0.68
FeO tot	6.55	7.31	5.31	5.36
MnO	0.13	0.16	0.13	0.22
MgO	15.51	14.72	15.35	15.77
CaO	21.34	18.83	21.24	21.42
Na_2O	0.83	1.11	0.71	0.86
K_2O	0.03	0.01	n.d.	0.02
Sum	101.79	99.41	100.58	101.26
Si	1.880	1.811	1.873	1.854
Al^{IV}	0.120	0.189	0.127	0.146
Al^{VI}	0.062	0.104	0.078	0.058
Fe^{3+}	0.074	0.099	0.031	0.096
Cr	0.001	0.005	0.022	0.019
Ti	0.033	0.047	0.028	0.033
Fe^{2+}	0.123	0.126	0.131	0.065
Mn	0.004	0.005	0.004	0.007
Mg	0.838	0.815	0.835	0.855
Ca	0.829	0.750	0.831	0.835
Na	0.058	0.080	0.050	0.061
K	0.001	0.001	0.000	0.001
Sum	4.024	4.031	4.010	4.031
Mol %				
Wo	43.025	39.984	44.145	43.494
En	43.502	43.485	44.395	44.565
Fs	10.451	12.275	8.799	8.771
Aeg	3.022	4.255	2.661	3.171
Species	Aug-Di	Aug	Aug	Aug-Di

n.d. not-detected

Table 4. Representative analyses of amphibole.

Sample	MC40	MC40	MC40	MC40	MC40	MC40	MC40	MC40	MC40	MC40	MC40	MC40	MC40
N. Analysis	3	5	6	7	27	28	29	43	44	45	46	4	9
Oxides (wt%)	rim	core	core	rim	rim	core	rim	rim	core	core	rim	rim/br Am*	rim/br Am*
SiO_2	44.02	45.93	45.70	52.99	49.98	51.03	50.42	41.63	45.43	46.42	44.42	56.24	54.27
TiO_2	3.38	2.90	2.79	0.62	0.43	0.34	0.35	0.58	0.69	0.29	0.42	0.08	0.12
Al_2O_3	9.54	8.43	8.60	2.96	6.69	5.36	6.64	13.08	10.30	9.07	12.01	6.37	6.30
Cr_2O_3	n.d.	n.d.	0.08	n.d.	0.06	n.d.	0.01	n.d.	0.02	n.d.	n.d.	n.d.	0.05
FeO tot	13.76	13.79	13.91	12.30	12.37	12.87	10.23	14.22	14.01	14.42	12.61	15.60	15.87
MnO	0.15	0.32	0.38	0.21	0.34	0.36	0.28	0.14	0.14	0.19	0.27	n.d.	0.19
MgO	12.82	13.81	13.92	15.30	17.38	17.52	17.55	12.76	12.96	14.75	13.72	9.95	11.08
CaO	10.25	10.14	10.19	12.15	9.84	8.98	10.97	10.76	11.49	10.20	11.16	2.50	4.97
Na_2O	2.90	2.55	2.61	0.96	1.87	1.53	1.78	2.62	2.51	1.60	2.71	5.62	4.74
K_2O	0.38	0.51	0.56	0.16	0.33	0.36	0.25	0.48	0.42	0.28	0.42	0.06	0.11
Sum	97.19	98.37	98.74	97.65	99.27	98.35	98.47	96.27	97.96	97.22	97.73	96.42	97.69
Si	6.464	6.602	6.550	7.636	6.857	6.999	7.013	6.115	6.617	6.593	6.408	7.975	7.688
Al^{IV}	1.536	1.398	1.450	0.364	1.081	0.866	0.987	1.885	1.383	1.407	1.592	0.025	0.312
Al^{VI}	0.114	0.029	0.002	0.138	0.000	0.000	0.100	0.379	0.385	0.110	0.450	1.039	0.739
Fe^{3+}	0.554	0.816	0.883	0.041	1.418	1.476	1.019	1.158	0.473	1.638	0.766	0.654	0.711
Ti	0.373	0.314	0.301	0.067	0.044	0.035	0.036	0.064	0.076	0.031	0.046	0.009	0.013
Cr	0.000	0.000	0.009	0.000	0.006	0.000	0.001	0.000	0.002	0.000	0.000	0.000	0.005
Fe^{2+}	1.135	0.841	0.785	1.440	0.000	0.000	0.171	0.588	1.234	0.075	0.755	1.195	1.169
Mn	0.019	0.039	0.046	0.026	0.040	0.042	0.033	0.017	0.017	0.022	0.033	0.000	0.023
Mg	2.806	2.960	2.974	3.287	3.554	3.582	3.640	2.793	2.815	3.123	2.950	2.104	2.340
Ca	1.612	1.561	1.564	1.876	1.447	1.319	1.635	1.693	1.793	1.552	1.725	0.380	0.755
Na	0.827	0.710	0.724	0.269	0.496	0.407	0.481	0.745	0.708	0.441	0.757	1.544	1.302
K	0.071	0.094	0.102	0.029	0.057	0.062	0.045	0.089	0.079	0.050	0.078	0.011	0.020
Sum	15.510	15.364	15.391	15.174	15.000	14.788	15.160	15.527	15.579	15.044	15.560	14.935	15.077
Species	Ts	Mg-Hbl	Mg-Hbl	Act	Mg-Hbl	Mg-Hbl	Mg-Hbl	Ts	Ed	Mg-Hbl	Ts	Glf	Win

n.d. not-detected

Table 5. Representative analyses of plagioclase.

Sample	MC40	MC40	MC40
N. Analysis	40	41	42
Oxides (wt%)	rim	core	rim
SiO_2	69.50	68.67	69.05
TiO_2	n.d.	n.d.	0.04
Al_2O3	19.88	19.76	19.70
Cr_2O3	0.01	n.d.	n.d.
FeO Tot	0.26	0.96	0.19
MnO	n.d.	0.03	n.d.
MgO	0.03	0.66	0.08
CaO	0.41	0.07	0.61
Na_2O	9.96	10.70	11.52
K_2O	0.04	0.03	0.04
Sum	100.07	100.88	101.24
Si	12.057	11.973	11.948
Al	4.063	4.06	4.017
Fe^{2+}	0.037	0.14	0.028
Ca	0.076	0.013	0.113
Na	3.349	3.616	3.863
K	0.008	0.007	0.009
Sum	19.59	19.809	19.979
An	2.218	0.353	2.844
Ab	97.546	99.451	96.927
Or	0.235	0.196	0.23

n.d. not-detected

saussuritized. Crystals display an intersertal texture and are pseudomorphosed by pumpellyite, prehnite, chlorite, and epidote.

Clinopyroxene (augite) (Table 3) is often twinned and shows wavy extinction. Chlorite, white mica, and green amphibole replace clinopyroxene. Minerals such as titanite, green and brown amphibole form coronas around clinopyroxene, indicative of ocean-floor metamorphism. Brown amphibole (c/γ 36°), sometimes twinned, also occurs in the metadolerites as isolated idioblasts; these minerals have rims of green amphiboles, opaque minerals, titanite, and orogenic blue amphibole.

Two types of green amphibole with different compositions are recognized: 1) a green hornblende occurs as single crystals and/or rims and coronas around brown hornblende or pyroxenes; 2) a pale green amphibole occurs in the veins or replaces clinopyroxene and has an actinolite composition (Table 4).

Blue amphibole forms rims and coronas after brown and/or green hornblende, and locally after clinopyroxene.

Chlorite occurs as fan-felt-radiated aggregates, sometimes overgrowing clinopyroxene or replacing amphibole.

Quartz occurs subordinately in these rocks and is found on the border of the clinopyroxene crystals in agreement with Cortesogno et al. (1994). Quartz shows dynamic recrystallization, deformation bands and sub-grain boundaries.

Pumpellyite aggregates are pseudomorph after plagioclase. Prehnite occurs as ovoid-fan-radiated aggregates, and shows a ductile deformation. White mica replaces clinopyroxene crystals.

Petrography of the veins

Veins are heterogeneous in texture and mineralogical composition, and show brittle (Figure 4) to ductile deformation (Figure 5). They are generally a few millimetres thick, and can be isolated or organised in closely spaced sets. Vein morphology ranges from planar, sinuous to irregular, with orientation that is slightly discordant to the metadolerite foliation, while minerals in the veins lack a preferred orientation. This indicates a syn- to post-kinematic vein formation with respect to the main foliation.

Veins are principally made of pumpellyite and other minerals such as ± chlorite ± prehnite ± plagioclase ± tremolite-actinolite ± white mica ± quartz ± calcite ± albite ± epidote ± lawsonite ± glaucophane and ± chrysotile.

Table 6. Representative analyses of pumpellyite.

Sample	MC40	MC40	MC40	MC40	MC40	MC40	MC40	MC81	MC77	MC77	MC77	MC77	MC70	MC70
N. Analysis	51	54	55	56	57	58	59	220	49	52	56	57	168	170
Oxides (wt%)	Veins	Veins	Veins	Veins	Veins	Veins	Veins	Veins	Veins	Veins	Veins	Veins	Veins	Veins
SiO_2	37.76	38.27	37.21	38.18	38.55	37.70	38.08	37.51	37.51	37.25	37.31	37.33	38.22	37.70
TiO_2	0.13	0.07	0.05	n.d.	0.03	0.01	0.05	0.07	0.13	0.05	0.04	0.07	0.07	0.06
Al_2O_3	25.12	24.51	23.67	26.08	24.22	23.97	25.21	24.41	23.18	22.68	24.96	24.07	25.74	26.04
Cr_2O_3	n.d.	0.04	0.01	n.d.	n.d.	0.08	0.05	n.d.	0.02	0.01	0.03	0.06	0.02	n.d.
FeO tot	4.47	4.39	5.14	3.95	4.36	5.05	2.92	4.27	6.04	7.43	3.38	5.49	2.83	3.18
MnO	0.07	0.11	0.18	0.07	0.08	0.18	0.04	0.08	0.10	0.10	0.23	0.11	0.21	0.24
MgO	2.64	2.92	2.80	2.16	3.15	2.68	3.17	2.89	2.45	2.54	2.98	2.31	3.43	3.17
CaO	23.31	23.03	23.49	23.26	23.10	23.15	23.53	22.46	22.06	22.22	22.22	22.35	22.20	22.52
Na_2O	0.04	0.06	0.08	0.01	0.05	0.05	0.06	0.06	0.03	0.04	0.07	0.03	0.09	0.08
K_2O	0.02	0.04	n.d.	n.d.	0.01	0.01	0.02	n.d.	n.d.	0.01	n.d.	n.d.	n.d.	n.d.
Sum	93.54	93.44	92.63	93.72	93.54	92.88	93.13	91.76	91.52	92.33	91.22	91.82	92.81	92.98
Si	3.459	3.504	3.468	3.472	3.524	3.493	3.477	3.493	3.532	3.509	3.478	3.496	3.484	3.443
Ti	0.009	0.005	0.003	0.000	0.002	0.001	0.003	0.005	0.009	0.004	0.003	0.005	0.005	0.004
Al	2.711	2.644	2.600	2.795	2.608	2.617	2.713	2.679	2.573	2.518	2.742	2.657	2.765	2.802
Cr	0.000	0.004	0.001	0.000	0.000	0.008	0.005	0.000	0.002	0.002	0.003	0.006	0.002	0.000
Fe^{2+}	0.342	0.336	0.401	0.301	0.333	0.391	0.223	0.332	0.476	0.585	0.263	0.430	0.216	0.243
Mn	0.005	0.009	0.014	0.005	0.006	0.014	0.003	0.007	0.008	0.008	0.018	0.009	0.016	0.018
Mg	0.361	0.399	0.389	0.293	0.430	0.370	0.431	0.401	0.344	0.357	0.414	0.323	0.466	0.432
Ca	2.287	2.259	2.345	2.265	2.262	2.298	2.302	2.241	2.226	2.242	2.219	2.243	2.168	2.203
Na	0.006	0.011	0.014	0.002	0.008	0.010	0.011	0.011	0.006	0.007	0.013	0.005	0.016	0.014
K	0.002	0.005	0.000	0.000	0.001	0.002	0.003	0.000	0.000	0.001	0.000	0.000	0.000	0.000
Sum	9.181	9.176	9.236	9.132	9.174	9.204	9.170	9.168	9.176	9.233	9.154	9.173	9.137	9.159

n.d. not-detected

Table 6. Continued ...

Sample	MC77	MC77	MC77	MC77	MC77	MC77	MC77	MC77	MC70
N. Analysis	64	78	79	83	49	101	102	115	161
	Pseudo-morphous after Pl	Pseudo-morphous after Pl	Pseudo-morphous after Pl	Pseudo-morphous after Pl	Pseudo-morphous after Pl	Pseudo-morphous after Pl	Pseudo-morphous after Pl	Pseudo-morphous after Pl	Pseudo-morphous after Pl
Oxides (wt%)									
SiO_2	37.64	38.33	37.72	41.00	37.85	37.82	37.98	38.40	38.05
TiO_2	0.08	0.06	0.06	0.04	0.06	0.02	0.03	0.03	0.10
Al_2O_3	25.04	25.12	25.40	24.37	25.02	25.58	25.63	25.31	25.36
Cr_2O_3	n.d.	n.d.	n.d.	n.d.	0.02	0.04	n.d.	n.d.	0.01
FeO tot	4.11	4.09	3.24	4.16	3.43	3.57	3.57	3.42	2.95
MnO	0.23	0.20	0.25	0.29	0.23	0.21	0.20	0.26	0.27
MgO	2.77	2.70	2.86	2.82	2.89	2.89	2.82	2.76	3.23
CaO	22.29	22.03	22.31	21.03	22.01	22.46	22.51	22.20	21.79
Na_2O	0.08	0.13	0.07	0.91	0.14	0.08	0.08	0.19	0.06
K_2O	n.d.	0.02	0.02	0.26	n.d.	n.d.	0.01	0.01	n.d.
Sum	92.24	92.68	91.94	94.89	91.64	92.68	92.82	92.58	91.83
Si	3.481	3.519	3.483	3.664	3.506	3.471	3.478	3.519	3.504
Ti	0.005	0.004	0.004	0.002	0.004	0.002	0.002	0.002	0.007
Al	2.729	2.718	2.764	2.567	2.732	2.766	2.766	2.734	2.753
Cr	0.000	0.000	0.000	0.000	0.002	0.004	0.000	0.000	0.001
Fe^{2+}	0.318	0.314	0.250	0.311	0.266	0.274	0.273	0.262	0.227
Mn	0.018	0.016	0.020	0.022	0.018	0.017	0.015	0.020	0.021
Mg	0.382	0.370	0.394	0.376	0.399	0.395	0.385	0.377	0.443
Ca	2.208	2.167	2.207	2.014	2.184	2.208	2.209	2.180	2.150
Na	0.015	0.023	0.013	0.158	0.024	0.014	0.014	0.033	0.010
K	0.000	0.003	0.002	0.030	0.000	0.000	0.001	0.001	0.001
Sum	9.157	9.132	9.138	9.144	9.136	9.152	9.144	9.129	9.118

n.d. not-detected

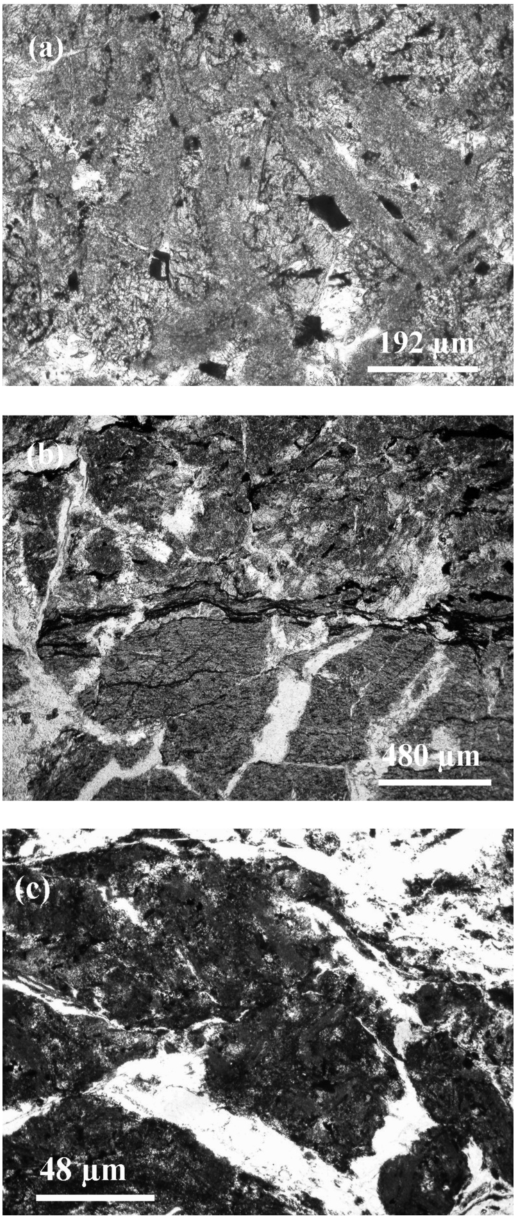

Figure 3. Textural features of metadolerites. (a) Intersertal texture; (b) blastophitic and mylonitic fabric; (c) veinscutting metadolerites. Plane-polarized light.

Pumpellyite occurs as felt-radiated aggregates and single isolated prismatic to acicular crystals, either in monomineralic veins (Figure 4) or in association with other minerals. The crystals show an undulose extinction and a ductile deformation. Pumpellyite is generally colourless, or shows a pale green-to-pale yellow grey and brown colour. In other cases they show a marked pleochroism from green to bluish green, displaying a typical birefringence colour in cross-polarized light, sometimes they show an anomalous interference colour. Chlorite flakes show an undulose extinction and occur as fan-felt-radiating aggregates (Figure 5).

Prehnite shows a ductile deformation and is usually found in association with chrysotile (Figure 6).

Plagioclase crystals have a granoblastic texture and show deformation twins as well as an undulose extinction. Plagioclase crystals have oligoclase (PL2) and albite (PL3) compositions.

Amphibole of actinolite composition occurs as nematoblasts and shows a ductile deformation. Isolated tiny crystals of blue amphibole may also occur in the veins. White mica occurs only as tiny flakes in the veins. Quartz shows undulose extinction and sometimes deformation bands, subgrain boundaries or evidence of new grain

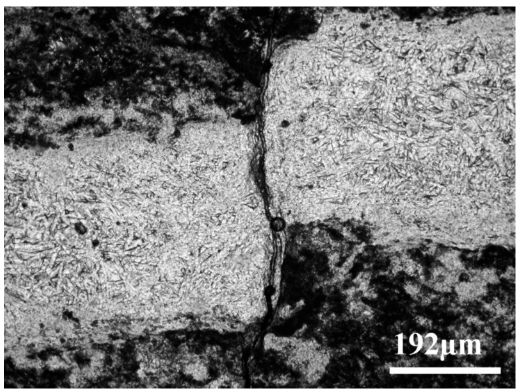

Figure 4. Pumpellyite vein displaced by microfault. Plane-polarized light.

crystallization and deformation recovery.

Calcite shows deformation twinning. Epidote mainly occurs as subidiomorphic crystals in plagioclase, chlorite, and actinolite crystals; they show both pale green and brown colours, and textures resulting from ductile deformation. Lawsonite occurs as small colourless crystals (Figure 7) and is associated to chlorite and pumpellyite. As already observed by Sansone et al. (2011), glaucophane forms rims developed at the expense of brown amphibole or as single tiny crystals. Chrysotile has a fibrous stretched subidiomorphic habit; it is colourless and associated to prehnite. Zircon, phosphates and sulphides are also enclosed in veins with pumpellyite and chlorite.

Small idiomorphic crystals of zircon, and xenomorphs of apatite and chalcopyrite may also be associated to pumpellyite and chlorite in the veins.

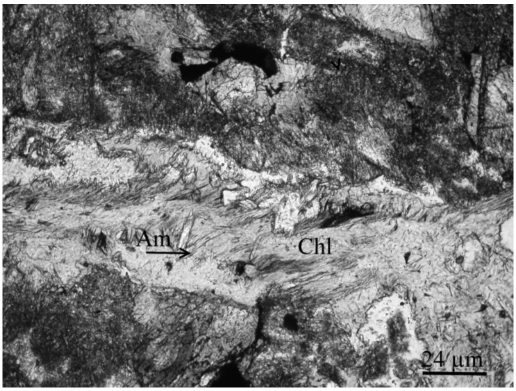

Figure 5. Vein with chlorite and amphibole. Plane-polarized light.

Composition of rocks and minerals

The metadolerite samples show N-MORB patterns (Sansone, 2010a; Sansone et al., 2011). The general inverse correlation between CaO and Na_2O (Table 2) suggests that the Ca-rich metadolerites were affected by rodingitic alteration, whereas Na-rich metadolerites suffered spilitic alteration, in agreement with ocean-floor and metasomatic metamorphic processes (Hart, 1970; Rollinson, 1993) and with previous results (Sansone et al., 2011).

In the metadolerites, the microstructures of clinopyroxenes are indicative of a relict magmatic phase, whereas those of amphibole and plagioclase phases of metamorphic and metasomatic processes (Sansone et al., 2011).

The structural formulas of clinopyroxenes (Table 3), calculated on the basis of 6 oxygens according to Morimoto (1988; 1989), show a progressive decreasing of augite from cores to rims; the diopsidic component follows an inverse trend.

The structural formulas of amphiboles (Table 4), based on 23 oxygens, encompasses different

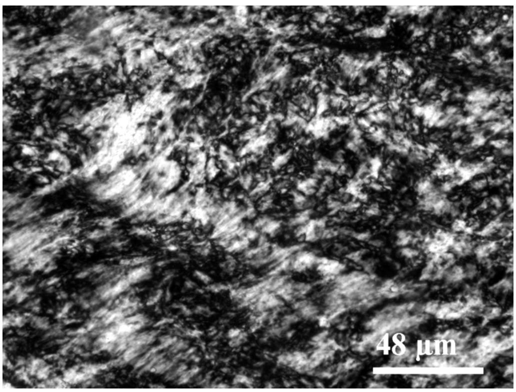

Figure 6. Prehnite vein. Crossed polars.

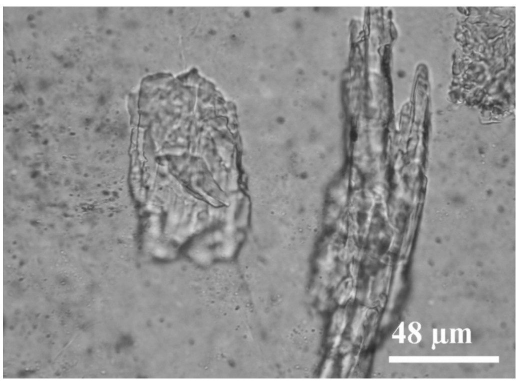

Figure 7. Lawsonite into vein. Plane-polarized light.

amphibole sub-groups, i.e. calcic, sodic and sodic–calcic (Leake et al., 1997; 2004). Green amphiboles ranges among edenite, actinolite, magnesiohornblende and tschermakite, whereas brown amphiboles among pargasite, magnesiohornblende and tschermakite; glaucophane and winchite systematically grow at the rims of brown amphiboles.

Plagioclases were recalculated on the basis of 32 oxygens as reported in Table 5; the magmatic plagioclase crystals are completely altered in the metadolerites, whereas the metamorphic plagioclases are albite-rich in composition.

The general formula of pumpellyite can be expressed in the form $W_2XY_2Z_3(O, OH)_{14}$ (Deer et al., 1994). The W site is occupied by Ca, Na and K whereas the Z site is occupied by Si. The X and Y are octahedral sites, where the X site is larger than the Y site. The X site is occupied by divalent and trivalent cations (Mg^{2+}, Al^{3+}, Mn^{2+}, Mn^{3+}, Fe^{2+}, Fe^{3+}, Cr^{3+}) whereas the Y site is occupied by trivalent cations (Al^{3+}, Fe^{3+}). The classification and nomenclature of pumpellyite have been largely based on the occupancy of the Y site (Passaglia and Gottardi, 1973): if the most abundant cation at the Y-site is Al, Fe^{3+}, Cr^{3+} and Mn^{3+} the corresponding pumpellyite end-memebers are pumpelliyte (Palache and Vassar, 1925), julgoldite (Moore, 1971), shuiskite (Ivanov et al., 1981) and okhotskite (Togari and Akasaka, 1987), respectively.

The crystal-chemical formulas of pumpellyites analysed in this study indicate that the Al end-member is by far the most abundant, the Fe^{3+} amount is small, whereas the Cr and Mn contents are negligible (Table 6). Moreover, the pumpelleyite are invariably Al-rich (Figure 8) and very close in composition irrespectively of their occurrence.

The linear and negative Fe and Al cotent correlation (Figure 9), evidences that in the veins the Fe content ranges between 0.216-0.585 and Al between 2.518-2.802 apfu, whereas pumpellyite pseudomorph shows Fe content up to 0.318.

SEM-BSE image shows that pumpellyite crystals are zoned with rims enriched in Al, Mg and depleted in Fe and Ca (Figure 10).

The core of pumpellyite crystals in the veins display a pale green pleochroism, while the rim is colourless; this variability could be correlated with the chemical composition and metamorphic conditions (Cortesogno et al., 1984 and reference therein). Pumpellyite pseudomorph after plagioclase is colourless.

Metamorphic evolution of the metadolerites

The metadolerites (Type A, B and C) from the Frido Unit Ophiolites (Southern Apennines - Italy) have been affected by an ocean-floor metamorphism under greenschist to amphibolite facies conditions and subsequent orogenic metamorphism under relatively HP/LT conditions (Sansone, 2010a; b; Sansone et al., 2011). Ocean-floor metamorphism often produced metasomatic reactions of rodingitization (Sansone et al., 2011).

Microscopic observations allow us to state that pumpellyite crystallised under high P and low T conditions in the veins, often in equilibrium with

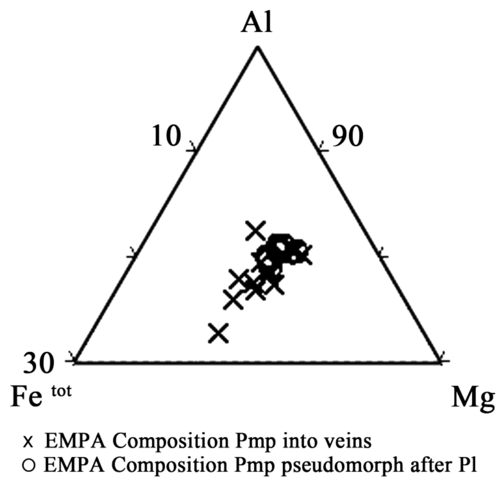

Figure 8. Composition of pumpellyite projected in the chemographic diagram Al, Fe^{tot}, Mg (atomic proportion).

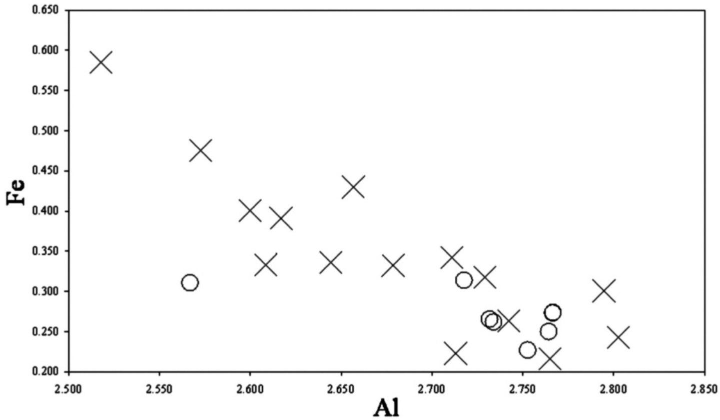

Figure 9. Fe vs Al (apfu) plot of pumpellyite. Cross for pumpellyite into veins; circle for pumpellyite pseudomorph after plagioclase.

lawsonite and glaucophane. The occurrence of prehnite in assemblage with pumpellyite indicates a retrograde metamorphic evolution. Pumpellyite in the veins is Fe-poor (0.216-0.585 apfu) and Al-rich (2.518-2.802 apfu). Pumpellyite pseudomorph after plagioclase shows Fe contents in the range 0.227-0.318 apfu and is Al-rich (2.567-2.766 apfu).

Al-pumpellyite in the veins cross-cutting metadolerites crystallised under conditions of the blueschist facies. It is known that temperature and pressure control the Al and Fe contents of pumpellyite: pumpellyite with Fe > 0.800 apfu crystallises in conditions of zeolite and prehnite-pumpellyite facies (Schiffman and Liou, 1980), while Al-pumpellyite crystallises under blueschist and pumpellyite-actinolite facies (AlDahan, 1986; Evans, 1990; Yuasa et al., 1992; Rahn et al., 1994; 1995). In the veins, pumpellyites associated with epidote contain less Fe and give information on the metamorphic conditions (Nakajima et al., 1977), suggesting that the rocks were altered at temperatures above the Fe pumpellyite stability curve (Liou, 1979).

BSE-SEM image in Figure 10 shows a zoned crystal of pumpellyite, with a Fe-rich core, and a Al-rich and Fe-poor rim, suggesting that the rim of these pumpellyite crystal formed during ocean-floor metamorphism, although Fe-content in pumpellyite is lower than that found in pumpellyite from other low-grade metamorphic rocks (Cortesogno et al., 1984). Al-rich rim suggests different metamorphic conditions typical of the pumpellyite-actinolite and blueschist facies condition. Therefore, the HP/LT orogenic

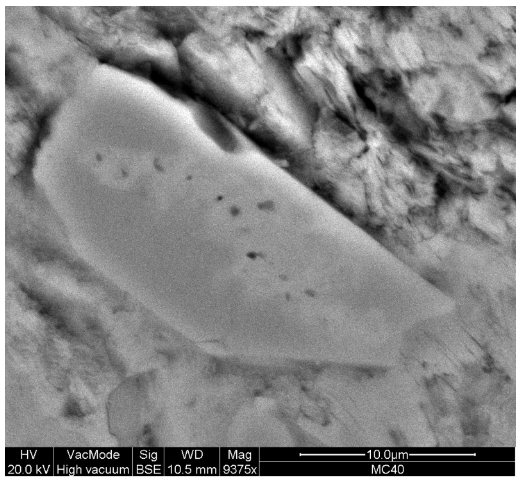

Figure 10. BSE image showing a zoned crystal of pumpellyite.

metamorphic event correlated to the underplating of the ophiolitic rocks situated at the base of the Liguride accretionary wedge, crystallised mineral assemblages typical of the lawsonite-glaucophane facies as also corroborated by the zoning of pumpellyite crystals. According to Knott (1994) and Sansone et al. (2011) this metamorphic facies developed at 6 - 8 kbar and 200-300 °C.

Pumpellyite compositions record the metamorphic evolution of the metadolerites (Type C), suggesting that both host rocks (pumpellyite pseudomorph after plagioclase) and pumpellyite filled veins shared the same metamorphic evolution. The occurrence of pumpellyite in assemblage with glaucophane, Mg-riebekite, lawsonite, phengite, pumpellyite and aegirine-augite (Sansone, 2010a; b) indicates that it crystallises under blueschist facies conditions.

Acknowledgements

Thanks go to G.B. Andreozzi and an anonymous reviewer for their helpful comments. The paper has benefited from the comments of Editor G. Iezzi to whom we are grateful.

References

AlDahan A.A. (1986) - Occurrence of epidote, pumpellyite and prehnite in Proterozoic clastics, dolerites and basalts from central Sweden. *Neues Jahrbuch für Mineralogie,* 155, 147-164.

Amodio-Morelli L., Bonardi G., Colonna V., Dietrich D., Giunta G., Ippolito F., Liguori V., Lorenzoni S., Paglianico A., Perrone V., Piccarreta G., Russo M., Scandone P., Zanettin-Lorenzoni E. and Zuppetta A. (1976) - L'arco Calabro-Peloritano nell'orogene Appenninico-Maghrebide. *Memorie della Società Geologica Italiana*, 17, 1-60.

Bonardi G., Amore F.O., Ciampo G., De Capoa P., Miconnét P. and Perrone V. (1988) - Il Complesso Liguride Auct.: Stato delle conoscenze attuali e problemi aperti sulla sua evoluzione Pre-Appenninica ed i suoi rapporti con l'Arco Calabro. *Memorie della Società Geologica Italiana*, 41, 17-35.

Bortolotti V. and Principi G. (2005) - Tethyan ophiolites and Pangea break-up. *The Island Arc*, 14, 442-470.

Cello G. and Mazzoli S. (1999) - Apennine tectonics in southern Italy: A review. *Journal of Geodynamics*, 27, 191-211.

Coombs D.S., Nakamura Y. and Vuagnat M. (1976) - Pumpellyite-actinolite facies schists of the Tayanne Formation near Loeche Valialis Switzerland. *Journal of Petrology*, 17, 440-471.

Cortesogno L., Lucchetti G. and Spadea P. (1984) - Pumpellyite in low-grade metamorphic rocks from Ligurian and Lucanian Apennines Maritime Alps and Calabria (Italy). *Contribution to Mineralogy and Petrology*, 85, 14-24.

Cortesogno L., Gaggero L. and Molli G. (1994) - Ocean floor tectono-metamorphic evolution in the Piedmont-Ligurian Jurassic basin: A review. *Memorie della Società Geologica Italiana*, 48, 151-163.

Deer W.A., Howie R.A. and Zussmann J. (1994) - Introduzione ai minerali che costituiscono le rocce. (eds): Zanichelli S.p.A, Bologna (Italy), 664 pp.

Doglioni C., Gueguen E., Harabaglia P. and Mongelli F. (1999) - On the origin of west-directed subduction zones and applications to the western Mediterranean. In: The Mediterranean basins: Tertiary extension within the alpine orogen. (eds): B. Durand, L. Jolivet, F. Horváth and M. Séranne, Special Publications Geological Society, London, 156, 541-561.

Ernst W.G., Seki Y., Onuki H and Gilbert M.C. (1970) - Comparative study of low-grade metamorphism in the California Coast Ranges and the outer metamorphic belt of Japan. *Geological Society of America Memoires*, 124, 276.

Evans B.W. (1990) - Phase relations of epidote blueschists. *Lithos*, 25, 3-23.

Franzini M., Leoni L. and Saitta M. (1972) - A simple method to evaluate the matrix effects in X-ray fluorescence analysis. *X-Ray Spectrom*, 1, 151-154.

Franzini M., Leoni L. and Saitta M. (1975) - Revisione di una metodologia analitica di fluorescenza-X basata sulla correzione completa degli effetti di matrice. *Rendiconti Società Italiana di Mineralogia e Petrologia*, 31, 365-378.

Gueguen E., Doglioni C. and Fernandez M. (1998) - On the post-25 Ma geodynamic evolution of the western Mediterranean. *Tectonophysics*, 298, 259-269.

Hart R. (1970) - Chemical exchange between seawater and deep ocean basalts. *Earth and Planetary Science Letters*, 9, 269-279.

Hellman P.L. and Henderson P. (1977) - Are rare earth elements mobile during spilitization? *Nature*, 267, 38-40.

Ishizuka H. (1991) - Pumpellyite from zeolite facies metabasites of the Horokanai ophiolite in the Kamuikotan zone, Hokkaido, Japan. *Contributions to Mineralogy and Petrology,* 107, 1-7.

Ivanov O.K., Arkhangel'skaya V.A., Miroshnikova L.O. and Shilova T.A. (1981) - Shuiskite, the chromium analogue of pumpellyite, from the Bisersk deposit, Urals. *Zapiski Vsesojuznogo Mineralogiceskogo Obscestva*, 110, 508-512.

Knott S.D. (1987) - The Liguride Complex of Southern Italy-a Cretaceus to Paleogene accretionary wedge. *Tectonophysics*, 142, 217-226.

Knott S.D. (1994) - Structure, kinematics and metamorphism in the Liguride Complex, Southern Apennine, Italy. *Journal of Structural Geology*, 16, 1107-1120.

Lanzafame G., Spadea P. and Tortorici L. (1979) - Mesozoic ophiolites of northern Calabria and Lucanian Apennine (Southern Italy). *Ofioliti*, 4, 173-182.

Leake B.E., Woolley A.R., Arps C.E.S., Birch W.D., Gilbert M.C., Grice J.D., Hawthorne F.C., Kato A., Kisch H.J., Krivovichev V.G., Linthout K., Laird J., Mandarino J.A., Maresch W.V., Nickel E.H., Rock N.M.S., Schumacher J.C., Smith D.C., Stephenson N.C.N., Ungaretti L., Whittaker E.J.W. and Youzhi G. (1997) - Nomenclature of amphiboles: Report of the Subcommittee on Amphiboles of the International Mineralogical Association, Commission on New Minerals and Mineral Names. *American Mineralogist*, 82, 1019-1037.

Leake B.E., Woolley A.R., Birch W.D., Burke E.A.J., Ferraris G., Grice J.D., Hawthorne F.C., Kisch H.J., Krivovichev V.G., Schumacher J.C., Stephenson N.C.N. and Whittaker E.J.W. (2004) - Nomenclature of amphiboles: Additions and revisions to the International Mineralogical Association's amphibole nomenclature. *American Mineralogist*, 89, 883-887.

Leoni L. and Saitta M. (1976) - Determination of yttrium and niobium on standard silicate rocks by X-ray fluorescence analysis. *X-Ray Spectrom*, 5, 29-30.

Liou J.G. (1979) - Zeolite facies metamorphism of basaltic rocks from the East Taiwan ophiolite. *American Mineralogist*, 64, 1-14.

Mazzoli S. (1998) - The Liguride units of southern Lucania (Italy): structural evolution and exhumation of high pressure metamorphic rocks. *Rendinconti Lincei*, 9, 271-291.

Mével C. (1981) - Occurrence of pumpellyite in hydrothermally altered basalts from the Vema Fracture Zone (Mid-Atlantic Ridge). *Contribution to Mineralogy and Petrology*, 76, 386-393.

Monaco C. (1993) - Le Unità Liguridi nel confine Calabro-Lucano (Appennino Meridionale): controllo dei dati esistenti, nuovi dati ed interpretazione. *Bollettino della Società Geologica Italiana,* 112, 751-769.

Monaco C., Tansi C., Tortorici L., De Franceso A.M. and Morten L. (1991) - Analisi geologico-strutturale dell'Unita` del Frido al confine calabro-lucano (Appennino Meridionale). *Memorie della Società Geologica Italiana*, 47, 341-353.

Monaco C. and Tortorici L. (1995) - Tectonic role of ophiolite-bearing terranes in building of the Southern Apennines orogenic belt. *Terra Nova*, 7, 153-160.

Monaco C., Tortorici L., Morten L., Critelli S., Tansi C. (1995) - Geologia del versante Nord-Orientale del Massiccio del Pollino (Confine Calabro Lucano): Nota illustrativa sintetica alla scala 1:50.000. *Bollettino della Società Geologica Italiana*, 114, 277-291.

Moore P.B. (1971) - Julgoldite, the Fe^{2+}- Fe^{3+} dominant pumpellyite. *Lithos*, 4, 93-99.

Morimoto N. (1988) - Nomenclature of pyroxenes. *Mineralogy and Petrology*, 39, 55-76.

Morimoto N. (1989) - Nomenclature of pyroxenes. *Canadian Mineralogist*, 27, 143-156.

Nakajima T., Banno S. and Suzuki T. (1977) - Reactions leading to the disappearance of pumpellyite in low grade metamorphic rocks of the Sanbagawa metamorphic belt in the Central Shikoku, Japan. *Journal of Petrology*, 18, 263-284.

Ogniben L. (1969) - Schema introduttivo alla geologia del confine calabro-lucano. *Memorie della Società Geologica Italiana*, 8, 453-763.

Palache C. and Vassar H.E. (1925) - Some minerals of the Keweenawan copper deposits: Pumpellyite a new mineral; sericite; saponite. *American Mineralogist*, 10, 412-418.

Passaglia E. and Gottardi G. (1973) - Crystal chemistry and nomenclature of pumpellyites and julgoldites. *Canadian Mineralogist*, 12, 219-223.

Patacca E. and Scandone P. (2007) - Geology of the southern Apennines. In: Results of the CROP Project, Sub-project CROP-04 Southern Apennines (Italy). (eds): A. Mazzotti, E. Patacca and P. Scandone. *Bollettino della Società Geologica Italiana*, Special Issue, 75-119.

Paulick H., Bach W., Godard M., De Hoog J.C.M., Suhr G. and Harvey J. (2006) - Geochemistry of abyssal peridotites (mid-Atlantic Ridge, 158200 N, ODP Leg 209): Implications for fluid/rock interaction in slow spreading environments. *Chemical Geology*, 234, 179-210.

Rahn M., Mullis J., Erdelbrock K. and Frey M. (1994) - Very low-grade metamorphism of the Taveyanne greywacke, Glarus Alps, Switzerland. *Journal of Metamorphic Geology*, 12, 625-641.

Rahn M., Mullis J., Erdelbrock K. and M. Frey (1995) - Alpine metamorphism in the North Helvetic Flysch of the Glarus Alps. *Eclogae Geologicae Helvetiae*, 88, 157-178.

Rollinson H.R. (1993) - Using geochemical data: evaluation, presentation, interpretation. (eds): Longman Group UK, 352 p.

Sansone M.T.C. (2010a) - Serpentiniti e metadoleriti dell'Unità del Frido: genesi, evoluzione e problematiche ambientali. Ph.D. Thesis, Università degli Studi della Basilicata, 158 pp.

Sansone M.T.C. (2010b) - Serpentinites and metadolerites from Frido Unit: genesis, evolution and environmental problems. *Plinius*, 36, 1-6.

Sansone M.T.C., Rizzo G. and Mongelli G. (2011) - Mafic rocks from ophiolites of the Liguride units (Southern Apennines): petrographical and geochemical characterization. *International Geology Review*, 53, 130-156.

Schiffman P. and Liou J.G. (1980) - Synthesis and stability relations of Mg-A1 pumpellyite, $Ca_4Al_5MgSi_6O_{21}(OH)_7$. *Journal of Petrology*, 21, 441-474.

Siivola J. and Schmid R. (2007) - List of mineral abbreviations. Recommendations by the IUGS Subcommission on the Systematics of Metamorphic Rocks: 12. Web version 01.02.07. IUGS Commission on the Systematics in Petrology.

Spadea P. (1979) - Contributo alla conoscenza dei metabasalti ofiolitici della Calabria Settentrionale e Centrale e dell'Appennino Lucano. *Rendiconti della Società Italiana di Mineralogia e Petrologia*, 35, 251-276.

Spadea P. (1982) - Continental crust rock associated with ophiolites in Lucanian Apennine (Southern Italy). *Ofioliti*, 7, 501-522.

Spadea P. (1994) - Calabria-Lucania ophiolites. *Bollettino di Geofisica Teorica ed Applicata*, 36, 271-281.

Stampfli G.M., Borel G.D., Marchant R. and Mosar J. (2002) - Western Alps geological constraints on western Tethyan reconstructions. In: Reconstruction of the evolution of the Alpine-Himalayan Orogen. (eds): G. Rosembaum and G.S. Lister, *Journal of Virtual Explorer*, 8, 77-106.

Togari K. and Akasaka M. (1987) - Okhotskite, a new mineral, an Mn^{3+} dominant member of the pumpellyite group, from the Kokuriki mine, Hokkaido, Japan. *Mineralogical Magazine*, 51, 611-614.

Tortorici L., Catalano S. and Monaco C. (2009) - Ophiolite-bearing mélanges in southern Italy. *Geological Journal*, 44, 153-166.

Vezzani L. (1969) - La Formazione del Frido (Neocomiano - Aptiano) tra il Pollino ed il Sinni. *Geologica Romana*, 8, 129-176.

Vezzani L. (1970) - Le ofioliti della zona tra Castelluccio Inferiore e S. Severino Lucano (Potenza). *Atti della Accademia Gioenia di Scienze Naturali in Catania*, 7, 1-49.

Yuasa M., Watanabe T., Kuwajima T., Hirama T. and Fujioka K. (1992) - Prehnite-pumpellyite facies metamorphism in oceanic arc basement from Site 791 in the Sumisu Rift, western pacific. In: Proceedings of the Ocean Drilling Program, Scientific Results, College Station, TX. (eds): Taylor B. and K. Fujioka et al., 126, 185-193.

Submitted, May 2011 - Accepted, February 2012